A Novel Methodology for the Design of Isophoric Phased Arrays

P. Rocca, N. Anselmi, A. Polo, and A. Massa

Contents

1 Irregular Phased Array Square ($2 \times 2, 4 \times 4$)-Tiling

1.1 Antenna Aperture: Rectangle 40×40 Elements

1.1.1 ISOPHORIC EXCITATIONS

Multi-Objective Optimization-based Tiling Method: ($m \times m, 2m \times 2m$)-BMTM NSGA-III

Array Analysis Parameters:

- Total Number of Elements: $J = 1600$.
- Spacing: $d = \lambda/2$;
- Number of Samples along u: 512;
- Number of Samples along v: 512;
- Tapering: Isophoric;
- Steering Direction:

Scan n.	θ_s	ϕ_s
1	0°	0°
2	5°	0°
3	5°	45°
4	5°	90°
5	5°	135°
6	5°	180°
7	5°	225°
8	5°	270°
9	5°	315°

Tiling Parameters:

- *Small* Tile: S_1-tile: 1×1;
- *Big* Tile: S_2-tile: 2×2;
- Clustering Ratio S_1-tile: $1 : 4$;
- Clustering Ratio S_2-tile: $1 : 16$;
- Total Number of Configurations: $\Gamma = 2.70 \times 10^{48}$;

NSGA-III Parameters:

- Population size: $P = 100$;
- Chromosome length: $l = 19$;
- Maximum number of generations: $K = 2000$;
- Maximum number of functional evaluation calls: $NFE = P \times K = 2.0 \times 10^5$;
- Objectives:
    1. Side-lobe Level: SLL [dB];
    2. Number of TRM: TRM;
- Number of initial Populations: $N_{pop} = 1$;
- Number of GA random Seeds: $N_{Seed} = 1$;
- Total number of Runs: $N_{Runs} = N_{pop} \times N_{Seed} = 1$;

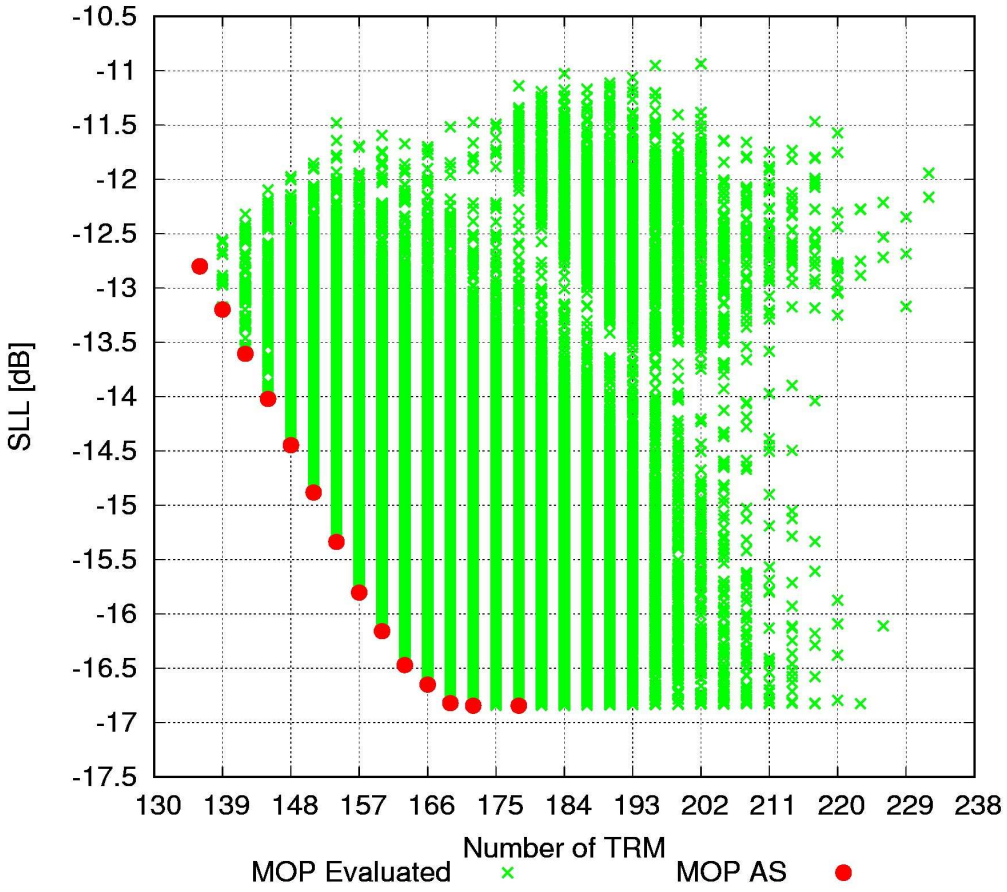

Figure 1: Numerical Assessment ($d_x = d_y = 0.5$ [λ], $k = 40$, $q = 40$, $J = 1600$) - Approximation Set: Objective 1 (SLL) vs. Objective 2 (Number of TRM).

Statistics

	Max	Min	Mean	Variance
SLL [dB]	-10.93	-16.84	-14.56	1.62

Table I: Runs Statistics

Number of TRM=178

Direction ($\theta = 0°, \phi = 0°$)

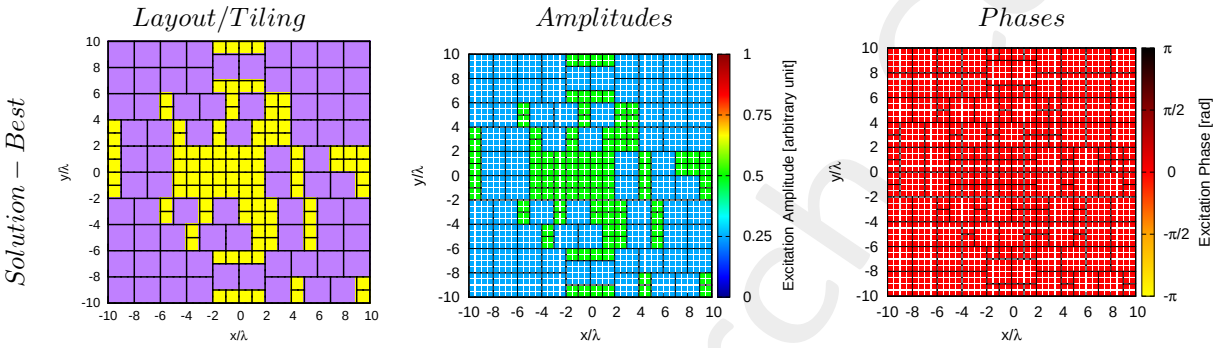

Figure 2: Numerical Assessment ($d_x = d_y = 0.5$ [λ], $k = 40$, $q = 40$, $J = 1600$) - Tiling configuration and weights coefficients value.

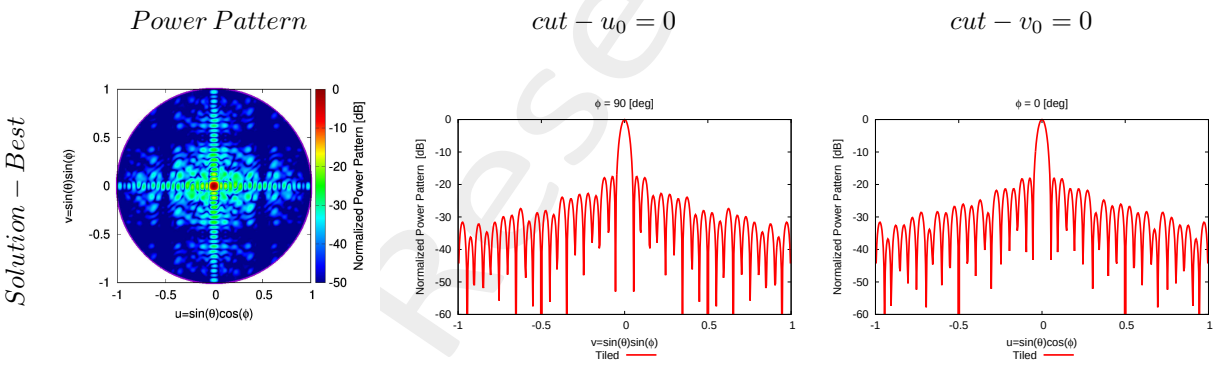

Figure 3: Numerical Assessment ($d_x = d_y = 0.5$ [λ], $k = 40$, $q = 40$, $J = 1600$) - Power patterns of the solutions.

	SLL [dB]	D [dBi]	$HPBW_{az}$ [deg]	$HPBW_{el}$ [deg]
$Solution - Best$	-17.55	36.40	2.66	2.66

Table II: Pattern descriptors for the presented solutions.

Direction ($\theta = 5°, \phi = 0°$)

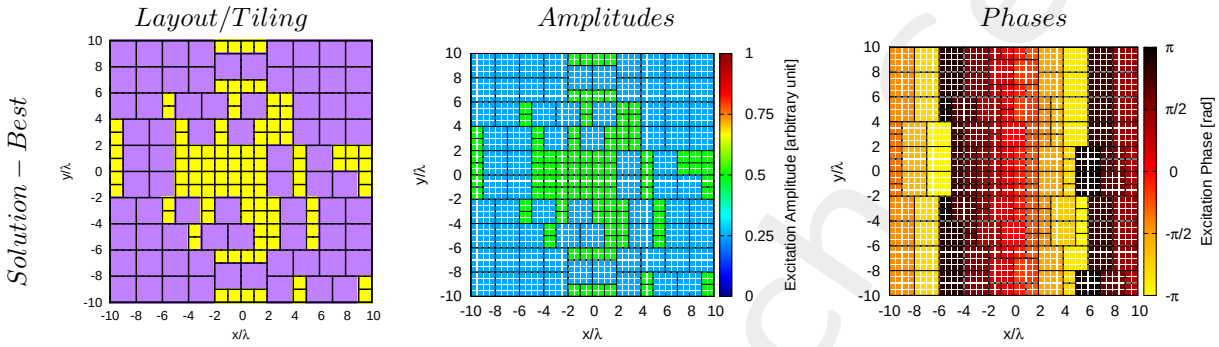

Figure 4: Numerical Assessment ($d_x = d_y = 0.5$ [λ], $k = 40$, $q = 40$, $J = 1600$) - Tiling configuration and weights coefficients value.

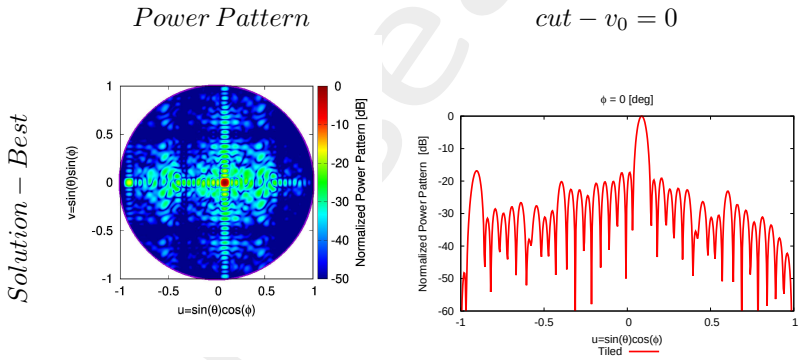

Figure 5: Numerical Assessment ($d_x = d_y = 0.5$ [λ], $k = 40$, $q = 40$, $J = 1600$) - Power patterns of the solutions.

	SLL [dB]	D [dBi]	$HPBW_{az}$ [deg]	$HPBW_{el}$ [deg]
$Solution - Best$	-16.85	36.00	2.68	2.67

Table III: Pattern descriptors for the presented solutions.

Direction ($\theta = 5°, \phi = 90°$)

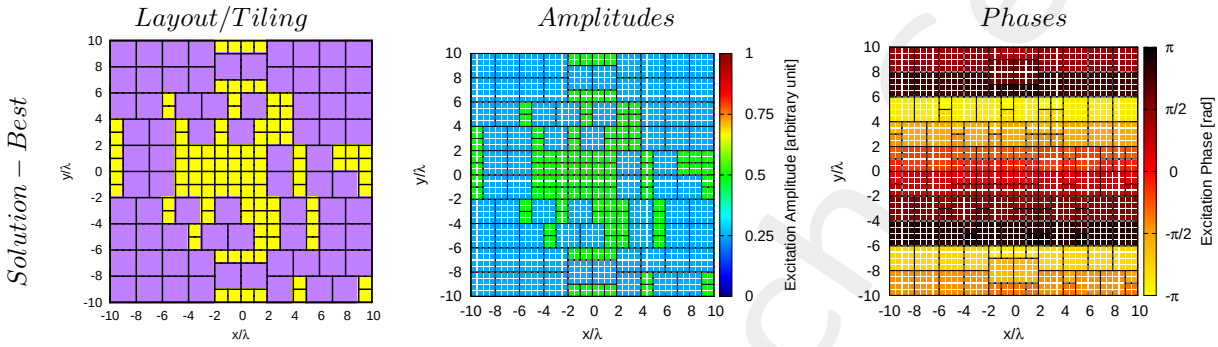

Figure 6: Numerical Assessment ($d_x = d_y = 0.5$ [λ], $k = 40$, $q = 40$, $J = 1600$) - Tiling configuration and weights coefficients value.

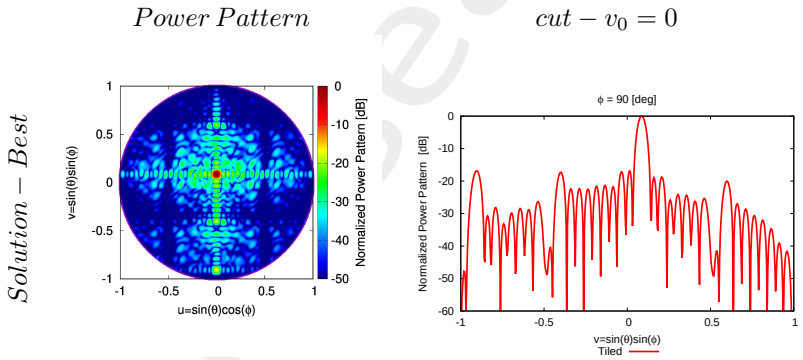

Figure 7: Numerical Assessment ($d_x = d_y = 0.5$ [λ], $k = 40$, $q = 40$, $J = 1600$) - Power patterns of the solutions.

	SLL [dB]	D [dBi]	$HPBW_{az}$ [deg]	$HPBW_{el}$ [deg]
$Solution - Best$	-16.84	36.00	2.68	2.67

Table IV: Pattern descriptors for the presented solutions.

2 Irregular Phased Array Square ($4 \times 4, 16 \times 16$)-Tiling

2.1 Antenna Aperture: Rectangle 120×120 Elements

2.1.1 ISOPHORIC EXCITATIONS

Optimization-based Tiling Method: ($m \times m, sm \times sm$)-BMTM Integer GA

Array Analysis Parameters:

- Total Number of Elements: $J = 14400$;
- Spacing: $d = \lambda/2$;
- Number of Samples along u: 512;
- Number of Samples along v: 512;
- Steering Direction: $(\theta_s, \phi_s) = \{(0°, 0°)\}$;
- Tapering: Isophoric;

Tiling Parameters:

- *Small* Tile: S_1-tile: 4×4;
- *Big* Tile: S_2-tile: 16×16;
- Clustering Ratio S_1-tile: $1 : 16$;
- Clustering Ratio S_2-tile: $1 : 256$;

GA Parameters:

- GA type: *Integer Genetic Algorithm.*
- Population size: $P = 50$;
- Crossover probability: $p_{CR} = 0.9$;
- Mutation probability: $p_M = 0.1$;
- Chromosome length: $l = 27$;
- Maximum number of generations: $K = 10000$;
- Maximum number of allowed TRM: $TRM = 900$;
- Maximum number of functional evaluation calls: $NFE = P \times K = 5.0 \times 10^5$;
- Number of initial Populations: $N_{pop} = 1$;
- Number of GA random Seeds: $N_{Seed} = 3$;
- Total number of Runs: $N_{Runs} = N_{pop} \times N_{Seed} = 3$;

NUMERICAL RESULTS

Number of TRM: 465

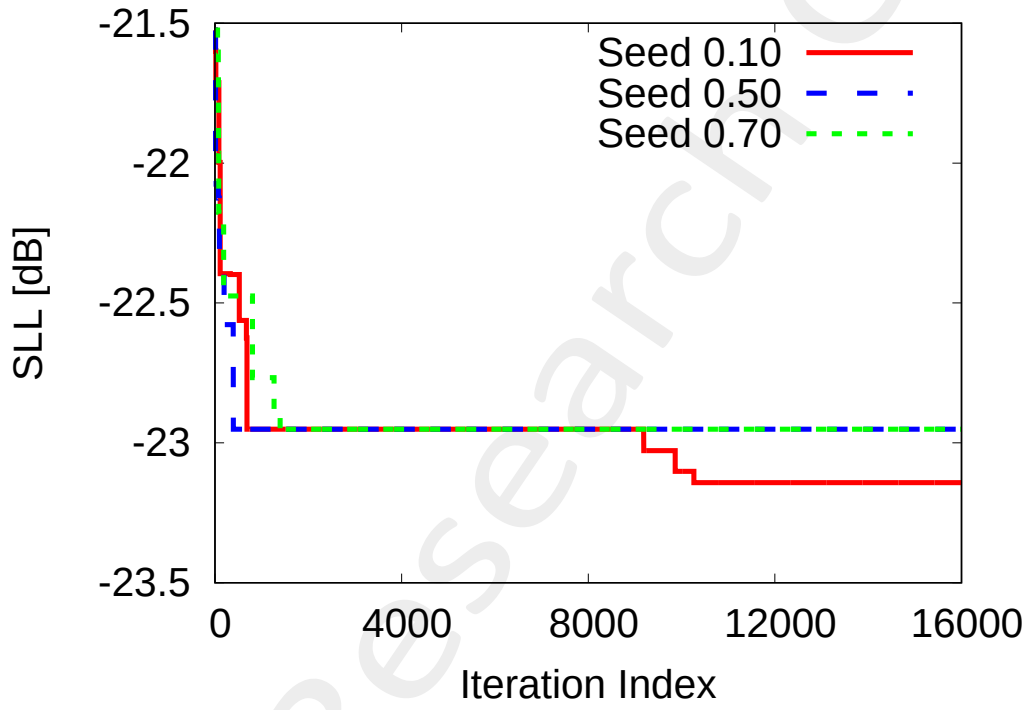

Figure 8: Numerical Assessment ($d_x = d_y = 0.5$ [λ], $k = 120$, $q = 120$, $J = 14400$) - SLL vs. Iterations.

Statistics

	Max	Min	Mean	Variance
SLL $[dB]$	-21.51	-23.10	-22.91	2.29×10^{-2}

Table V: Runs Statistics

Direction ($\theta = 0°, \phi = 0°$)

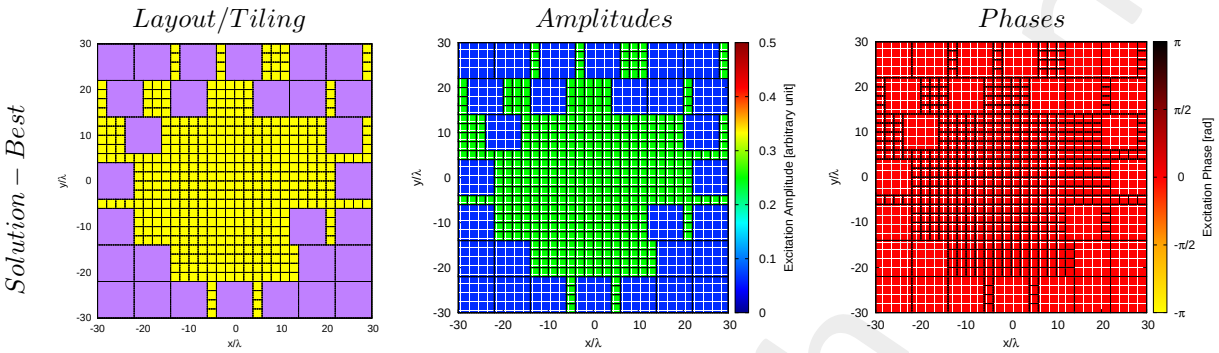

Figure 9: Numerical Assessment ($d_x = d_y = 0.5$ [λ], $k = 120$, $q = 120$, $J = 14400$) - Tiling configuration and weights coefficients value.

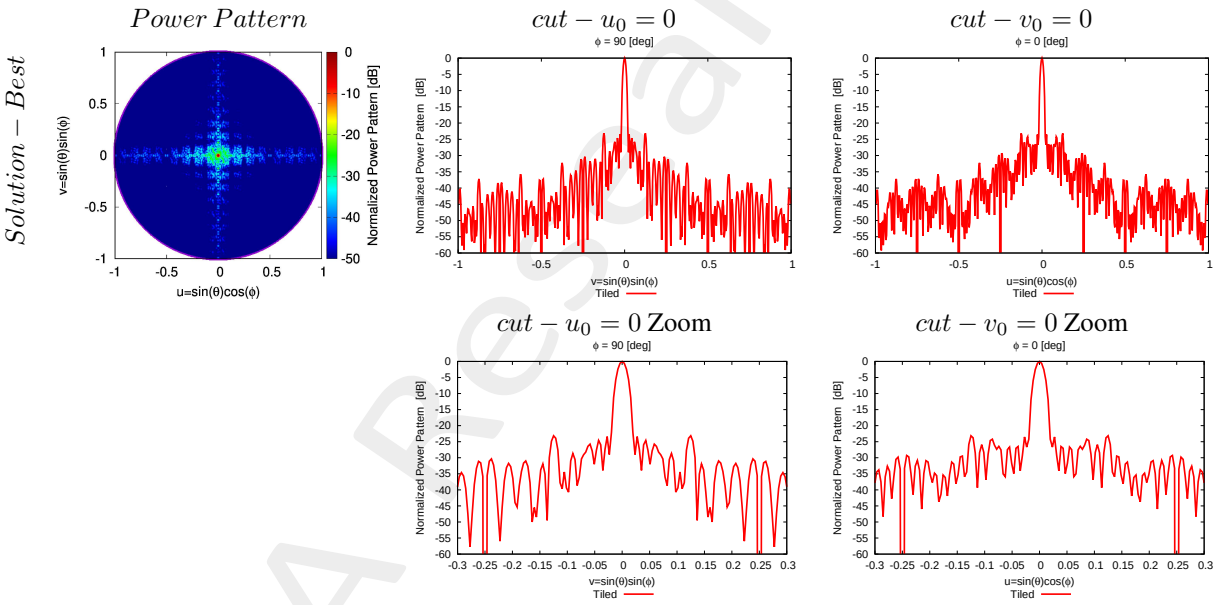

Figure 10: Numerical Assessment ($d_x = d_y = 0.5$ [λ], $k = 120$, $q = 120$, $J = 14400$) - Power patterns of the solutions.

	SLL [dB]	D [dBi]	$HPBW_{az}$ [deg]	$HPBW_{el}$ [deg]
$Solution - Best$	-23.10	45.12	0.98	1.00

Table VI: Pattern descriptors for the presented solutions.

Direction ($\theta = 5°, \phi = 0°$)

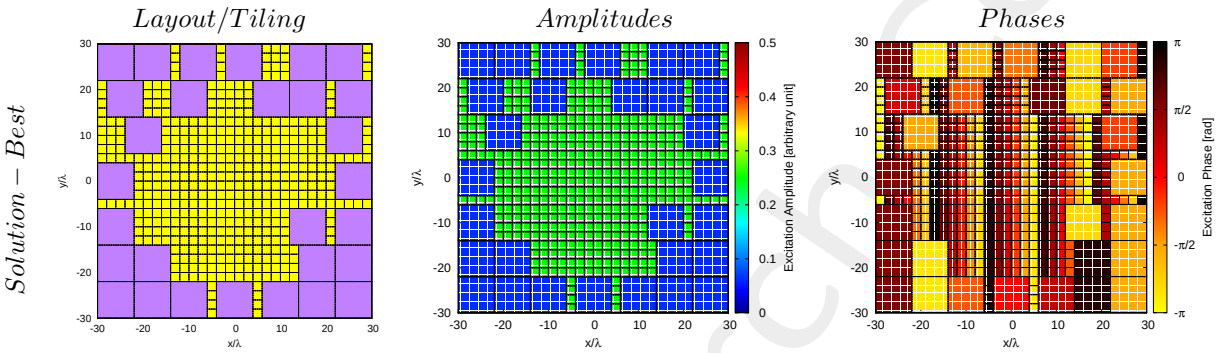

Figure 11: Numerical Assessment ($d_x = d_y = 0.5$ [λ], $k = 120$, $q = 120$, $J = 14400$) - Tiling configuration and weights coefficients value.

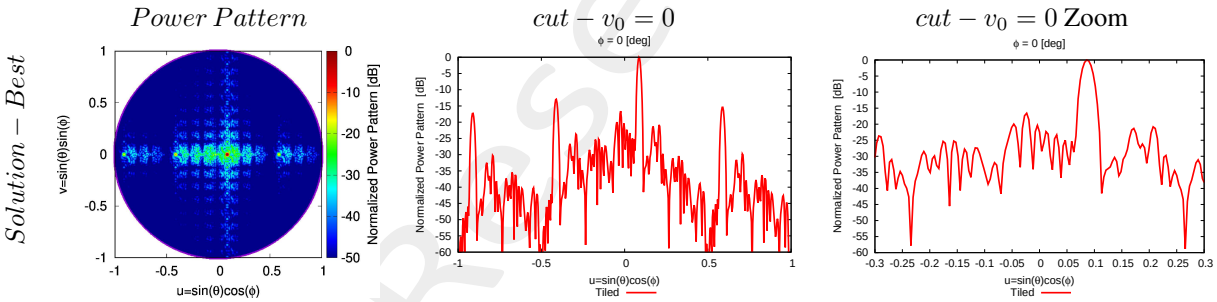

Figure 12: Numerical Assessment ($d_x = d_y = 0.5$ [λ], $k = 120$, $q = 120$, $J = 14400$) - Power patterns of the solutions.

	SLL [dB]	D [dBi]	$HPBW_{az}$ [deg]	$HPBW_{el}$ [deg]
$Solution - Best$	-12.93	43.34	1.05	1.08

Table VII: Pattern descriptors for the presented solutions.

Direction ($\theta = 5°, \phi = 90°$)

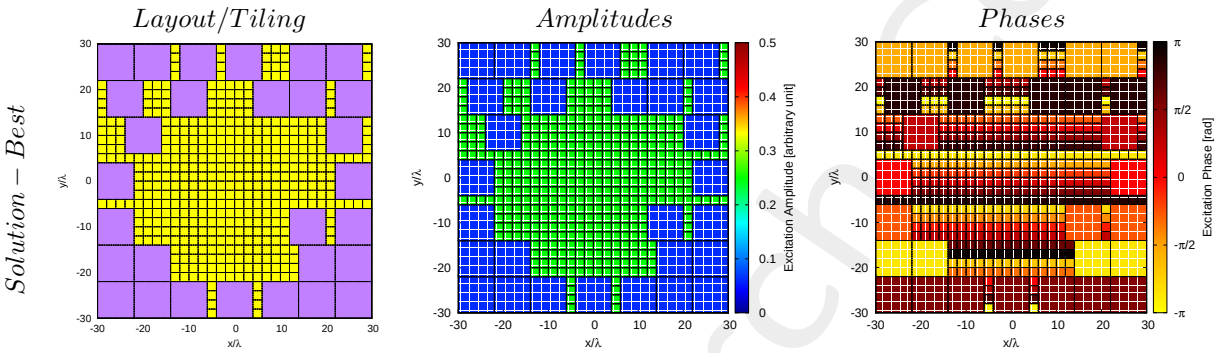

Figure 13: Numerical Assessment ($d_x = d_y = 0.5$ [λ], $k = 120$, $q = 120$, $J = 14400$) - Tiling configuration and weights coefficients value.

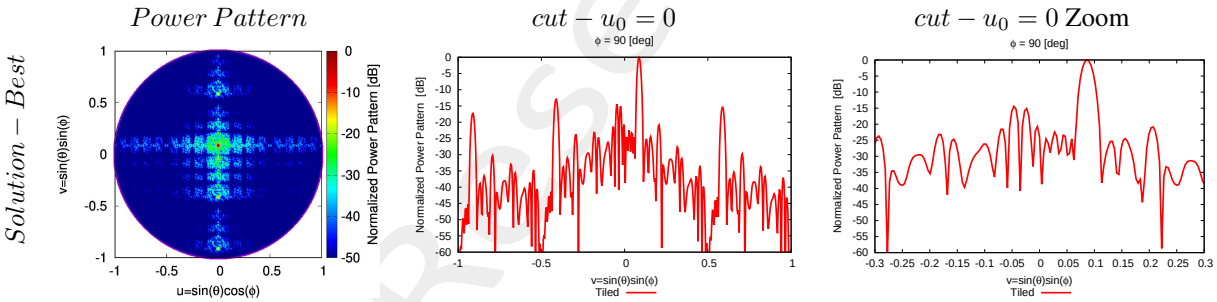

Figure 14: Numerical Assessment ($d_x = d_y = 0.5$ [λ], $k = 120$, $q = 120$, $J = 14400$) - Power patterns of the solutions.

	SLL [dB]	D [dBi]	$HPBW_{az}$ [deg]	$HPBW_{el}$ [deg]
$Solution - Best$	-12.92	43.34	1.04	1.09

Table VIII: Pattern descriptors for the presented solutions.

3 Comparative Results

3.1 ETM - Domino Tiling vs. $(1 \times 1, 2 \times 2)$-Tiling: Non-Isophoric Excitations

3.1.1 Antenna Aperture Rectangle 5×8 Elements

Array Analysis Parameters:

- Total Number of Elements: $J = 40$;
- Spacing: $d = \lambda/2$;
- Number of Samples along u: 256;
- Number of Samples along v: 256;
- Steering Direction: $(\theta_s, \phi_s) = \{(0°, 0°)\}$;
- Tapering: CP - Symmetric Mask;
- Main Lobe Window Width along u: $MW_u = 0.7$ [u];
- Main Lobe Window Width along v: $MW_v = 1.10$ [v];
- Side Lobe levels: $SLL_1 = -30$ [dB];

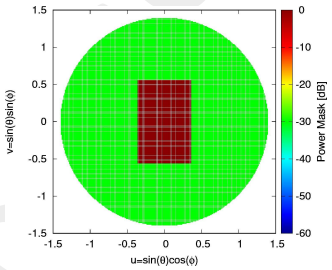

Figure 15: The power pattern mask used for the reference tapering optimization with CP.

Domino Tiling Parameters:

- Tile: Domino;
- Clustering Ratio: $1:2$;
- Total Number of Configurations: $\Gamma = 14824$;

$(1 \times 1, 2 \times 2)$**-Tiling Parameters:**

- *Small* Tile: S_1-tile: 1×1;
- *Big* Tile: S_2-tile: 2×2;
- Clustering Ratio S_1-tile: $1:1$;
- Clustering Ratio S_2-tile: $1:4$;
- Total Number of Configurations: $\Gamma = 16334$;

NUMERICAL RESULTS

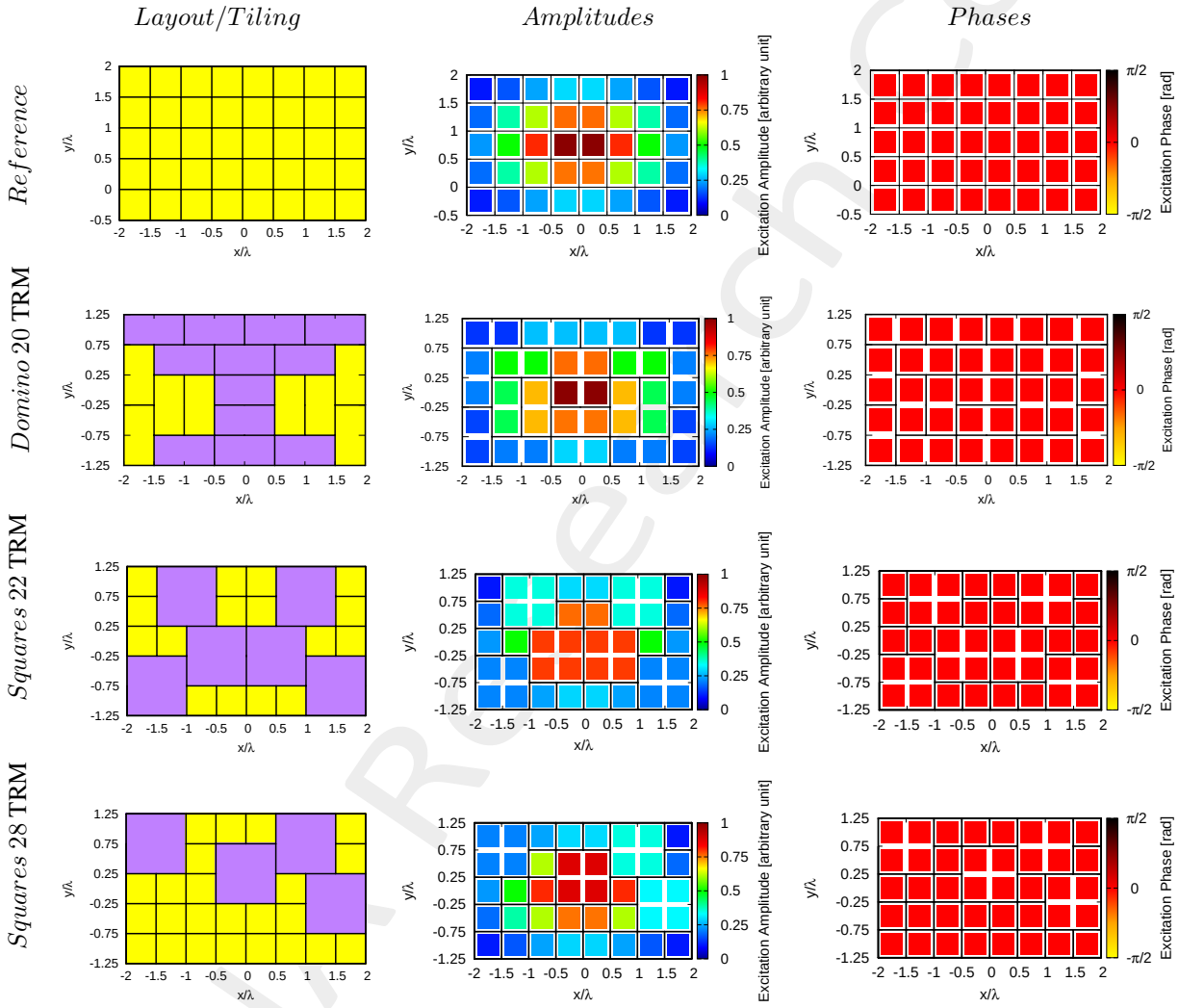

Figure 16: Numerical Assessment ($d_x = d_y = 0.5$ [λ], $k = 5$, $q = 8$, $J = 40$) - Tiling configuration and weights coefficients value.

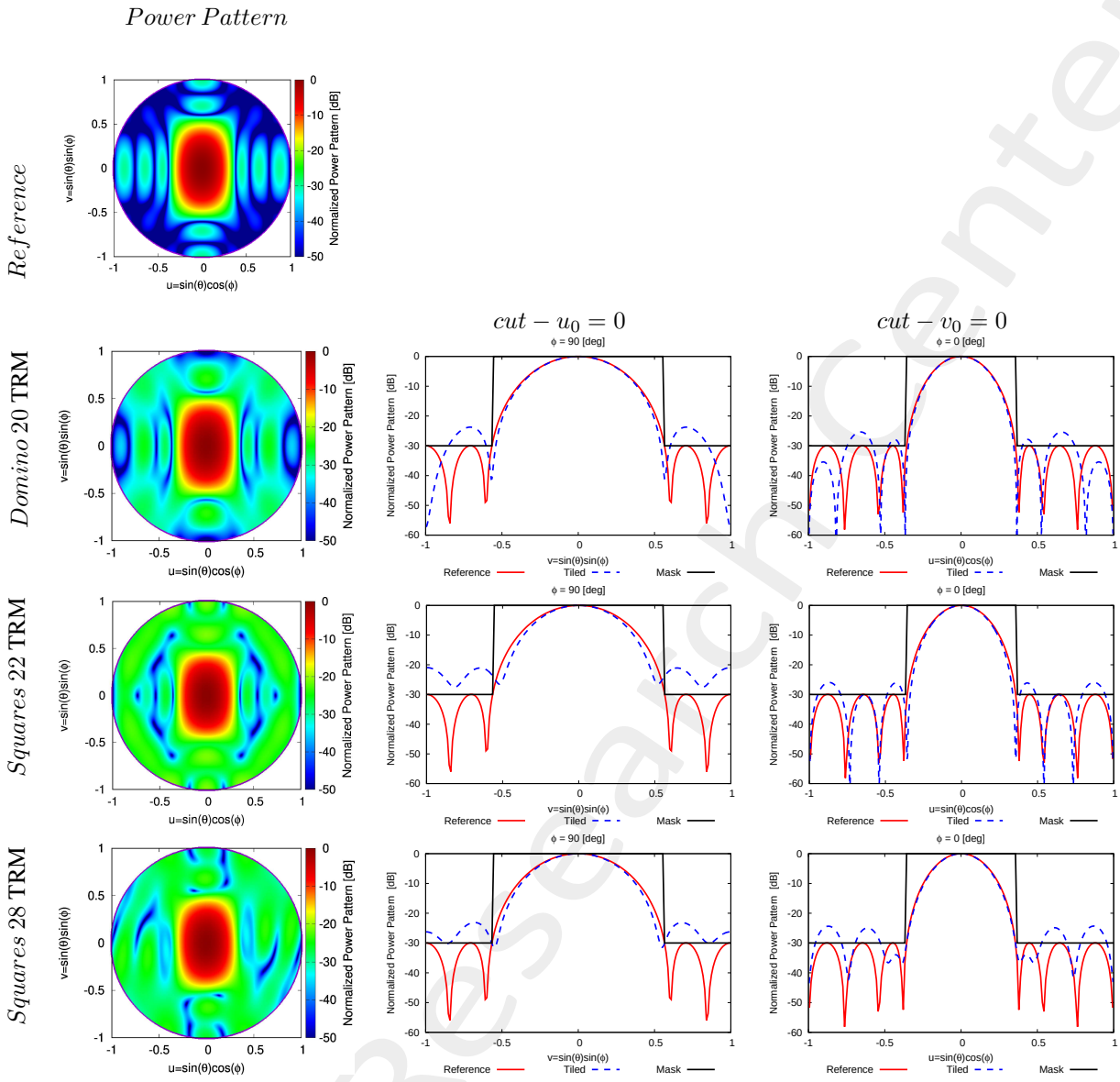

Figure 17: Numerical Assessment ($d_x = d_y = 0.5$ [λ], $k = 5$, $q = 8$, $J = 40$) - Power patterns of the solutions.

	SLL [dB]	D [dBi]	$HPBW_{az}$ [deg]	$HPBW_{el}$ [deg]	TRM
$Reference$	-29.93	$19,36$	16.43	26.39	40
$Domino$	-23.73	19.39	16.15	25.96	20
$Squares$	-20.94	19.37	15.88	24.46	22
$Squares$	-23.08	19.40	16.02	25.31	28

Table IX: Pattern descriptors for the presented solutions.

3.2 ETM - Domino Tiling vs. Squares Tiling: Isophoric Excitations

3.2.1 Antenna Aperture Rectangle 5×8 Elements

Array Analysis Parameters:

- Total Number of Elements: $J = 40$;
- Spacing: $d = \lambda/2$;
- Number of Samples along u: 256;
- Number of Samples along v: 256;
- Steering Direction: $(\theta_s, \phi_s) = \{(0°, 0°)\}$;
- Tapering: Isophoric;

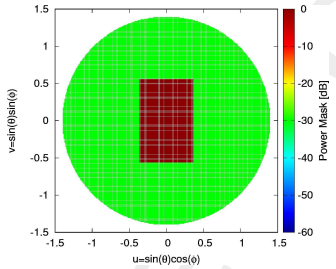

Figure 18: The power pattern mask used for the reference tapering optimization with CP.

Domino Tiling Parameters:

- Tile: Domino;
- Clustering Ratio: $1 : 2$;
- Total Number of Configurations: $\Gamma = 14824$;

(1×1, 2×2)-Tiling Parameters:

- *Small* Tile: S_1-tile: 1×1;
- *Big* Tile: S_2-tile: 2×2;
- Clustering Ratio S_1-tile: $1 : 1$;
- Clustering Ratio S_2-tile: $1 : 4$;
- Total Number of Configurations: $\Gamma = 16334$;

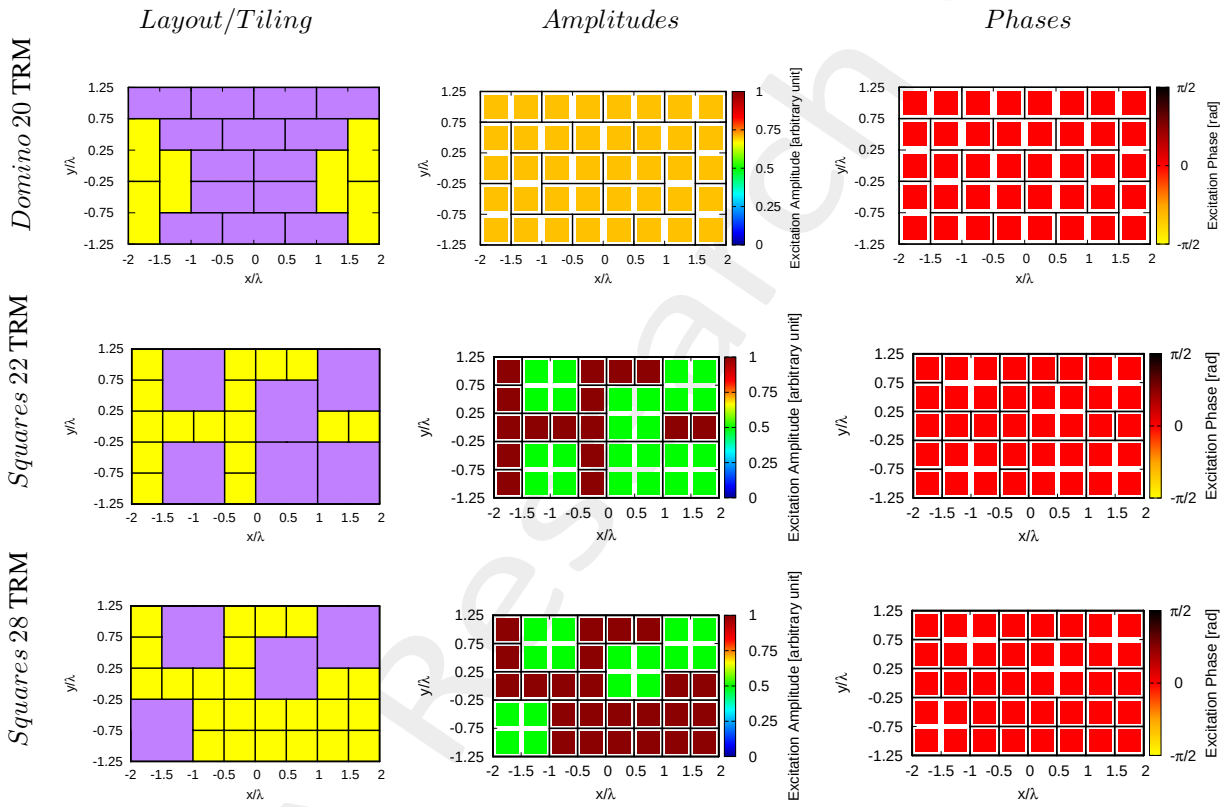

Figure 19: Numerical Assessment ($d_x = d_y = 0.5$ [λ], $k = 5$, $q = 8$, $J = 40$) - Tiling configuration and weights coefficients value.

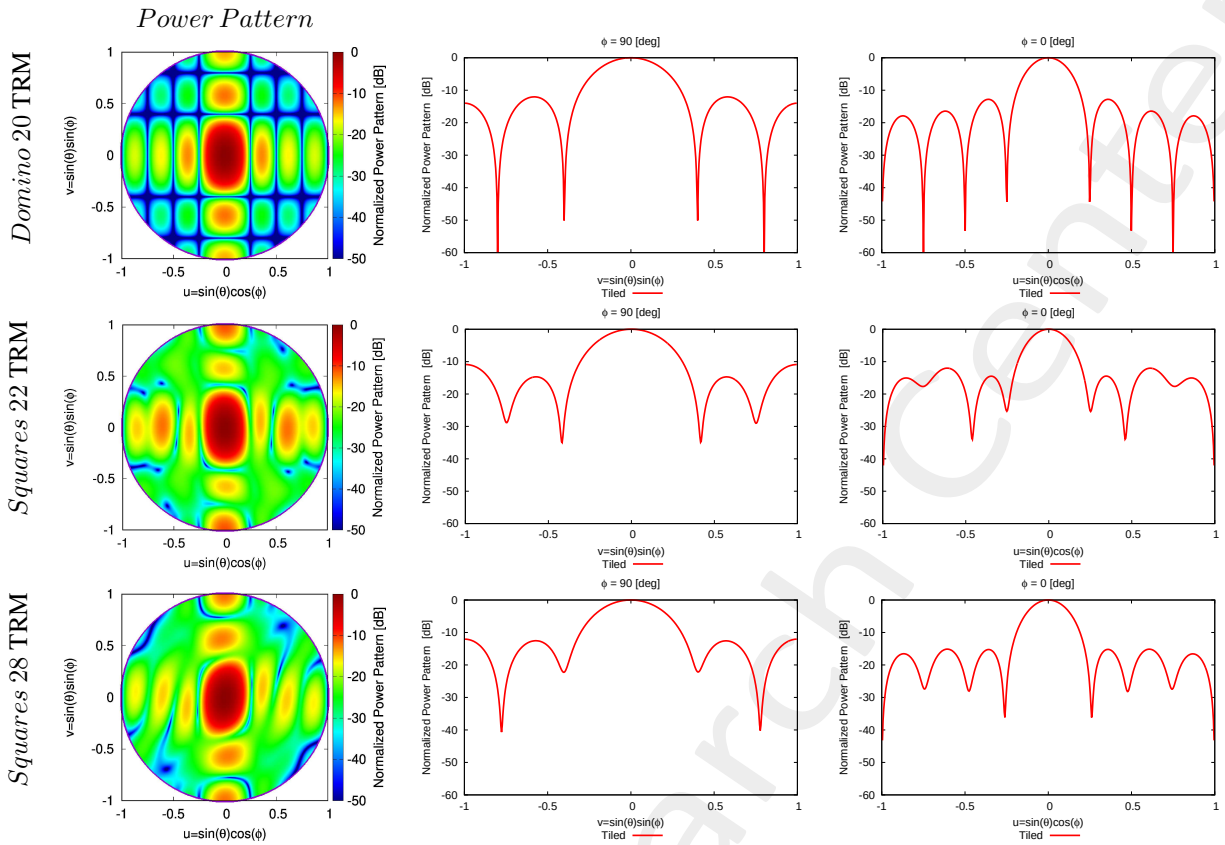

Figure 20: Numerical Assessment ($d_x = d_y = 0.5$ [λ], $k = 5$, $q = 8$, $J = 40$) - Power patterns of the solutions.

	SLL [dB]	D [dBi]	$HPBW_{az}$ [deg]	$HPBW_{el}$ [deg]	TRM
Domino	−12.04	20.49	12.08	20.77	20
Squares	−10.88	19.61	12.75	21.24	22
Squares	−12.04	19.90	13.07	20.89	28

Table X: Pattern descriptors for the presented solutions.

3.3 Isophoric: n−tile Edge Size Analysis

3.3.1 Antenna Aperture Rectangle 25×25 Elements

Optimization-based Tiling Method: Integer GA

Array Analysis Parameters:

- Total Number of Elements: $J = 625$;
- Spacing: $d = \lambda/2$;
- Number of Samples along u: 512;
- Number of Samples along v: 512;
- Steering Direction: $(\theta_s, \phi_s) = \{(0°, 0°)\}$;
- Tapering: Isophoric;

Tiling Parameters:

- *Small* Tile: S_1-tile: 1×1;
- *Big* Tile: S_2-tile: 2×2;
- Clustering Ratio S_1-tile: $1:1$;
- Clustering Ratio S_2-tile: $\{1:4,\ 1:9,\ 1:16,\ 1:25,\ 1:36\}$;

GA Parameters:

- GA type: *Integer Genetic Algorithm;*
- Population size: $P = 60$;
- Crossover probability: $p_{CR} = 0.9$;
- Mutation probability: $p_M = 0.1$;
- Chromosome length: $l = 20 - 24$;
- Maximum number of generations: $K = 20000$;
- Maximum number of allowed TRM: $TRM = 625$;
- Maximum number of functional evaluation calls: $NFE = P \times K = 1.2 \times 10^6$;
- Number of initial Populations: $N_{pop} = 1$;
- Number of GA random Seeds: $N_{Seed} = 18$;
- Total number of Runs: $N_{Runs} = N_{pop} \times N_{Seed} = 18$;

NUMERICAL RESULTS

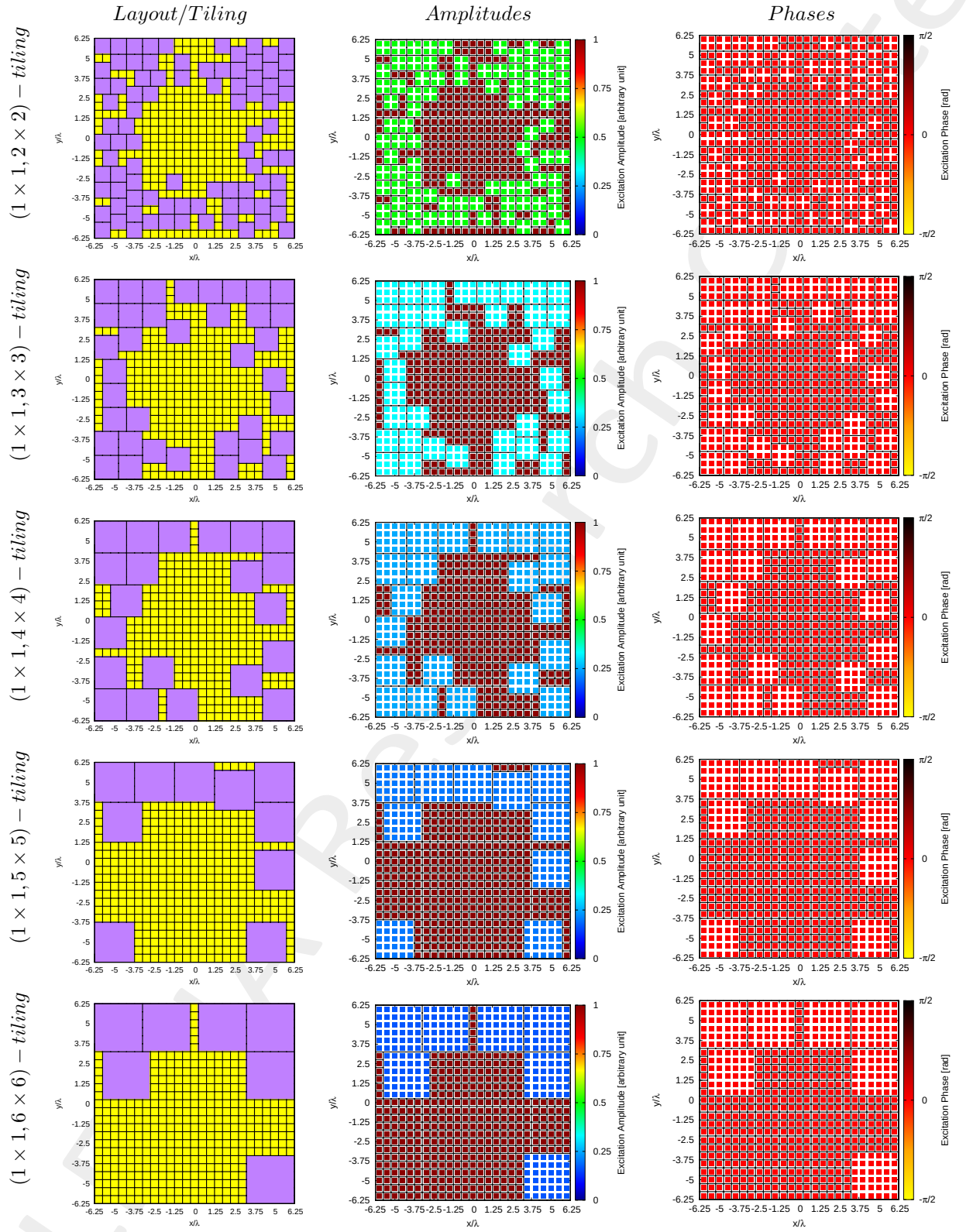

Figure 21: Numerical Assessment ($d_x = d_y = 0.5$ [λ], $k = 25$, $q = 25$, $J = 625$) - Tiling configuration and weights coefficients value.

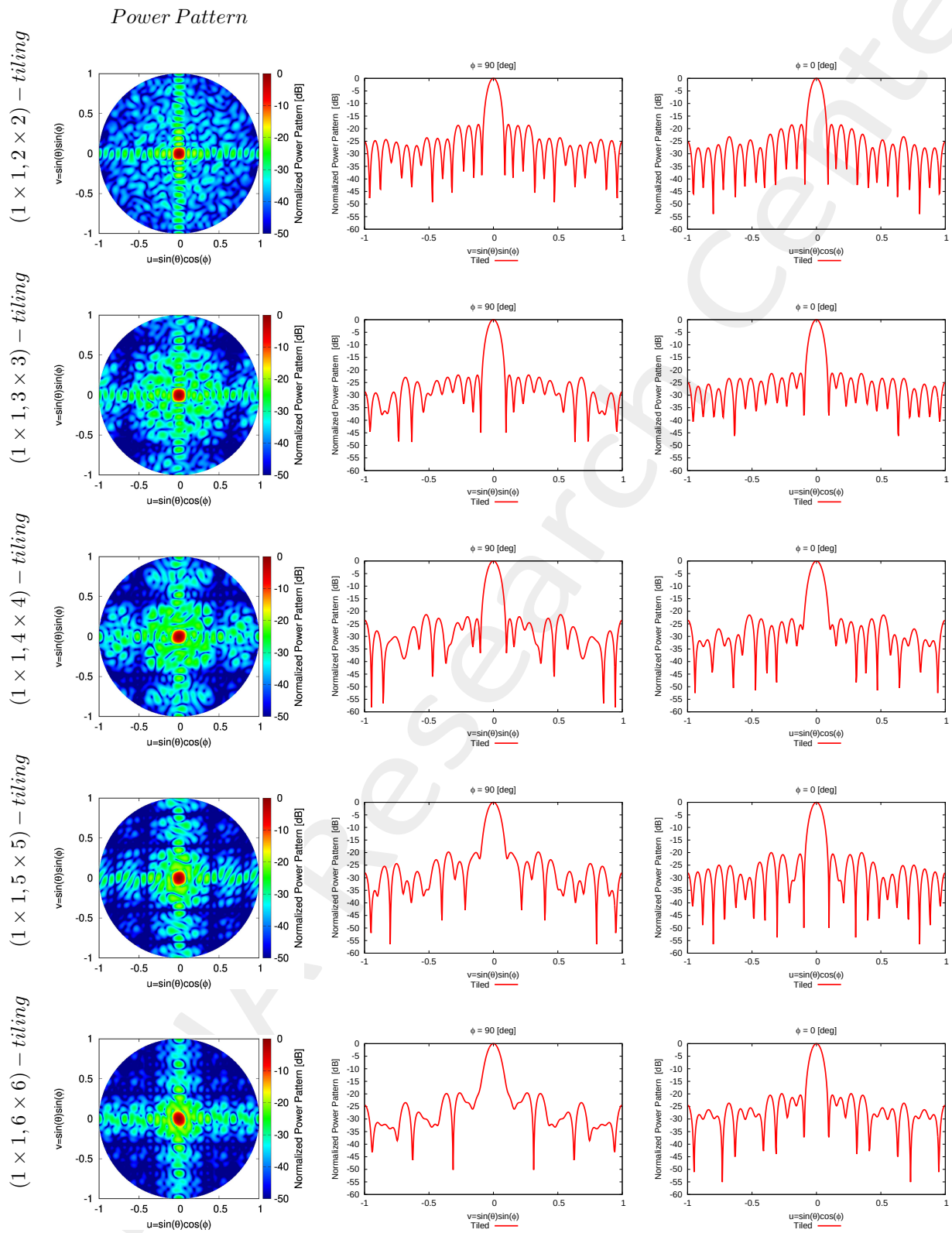

Figure 22: Numerical Assessment ($d_x = d_y = 0.5$ [λ], $k = 25$, $q = 25$, $J = 625$) - Power patterns of the solutions.

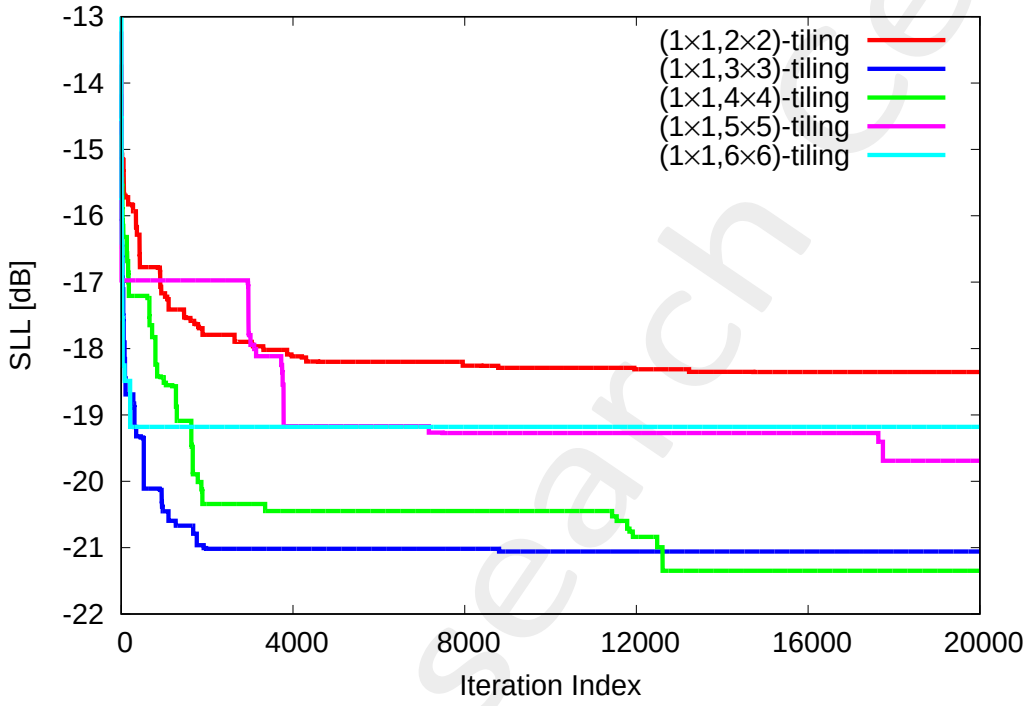

Figure 23: Numerical Assessment ($d_x = d_y = 0.5$ [λ], $k = 25$, $q = 25$, $J = 625$) - SLL vs. Iterations.

	SLL [dB]	D [dBi]	$HPBW_{az}$ [deg]	$HPBW_{el}$ [deg]	TRM
$(1 \times 1, 2 \times 2) - tiling$	-18.35	32.14	4.29	4.28	364
$(1 \times 1, 3 \times 3) - tiling$	-21.05	31.57	4.47	4.57	329
$(1 \times 1, 4 \times 4) - tiling$	-21.34	31.17	4.71	4.71	310
$(1 \times 1, 5 \times 5) - tiling$	-19.69	31.44	4.57	4.82	385
$(1 \times 1, 6 \times 6) - tiling$	-19.17	31.30	4.49	4.98	380

Table XI: Pattern descriptors for the presented solutions.

3.3.2 Antenna Aperture Rectangle 30×30 Elements

Optimization-based Tiling Method: Integer GA

Array Analysis Parameters:

- Total Number of Elements: $J = 900$;
- Spacing: $d = \lambda/2$;
- Number of Samples along u: 512;
- Number of Samples along v: 512;
- Steering Direction: $(\theta_s, \phi_s) = \{(0°, 0°)\}$;
- Tapering: Isophoric;

Tiling Parameters:

- *Small* Tile: S_1-tile: 1×1;
- *Big* Tile: S_2-tile: 2×2;
- Clustering Ratio S_1-tile: $1 : 1$;
- Clustering Ratio S_2-tile: $\{1 : 4,\ 1 : 9,\ 1 : 16,\ 1 : 25,\ 1 : 36\}$;

GA Parameters:

- GA type: *Integer Genetic Algorithm;*
- Population size: $P = 60$;
- Crossover probability: $p_{CR} = 0.9$;
- Mutation probability: $p_M = 0.1$;
- Chromosome length: $l = 25 - 29$;
- Maximum number of generations: $K = 20000$;
- Maximum number of allowed TRM: $TRM = 900$;
- Maximum number of functional evaluation calls: $NFE = P \times K = 1.2 \times 10^6$;
- Number of initial Populations: $N_{pop} = 1$;
- Number of GA random Seeds: $N_{Seed} = 18$;
- Total number of Runs: $N_{Runs} = N_{pop} \times N_{Seed} = 18$;

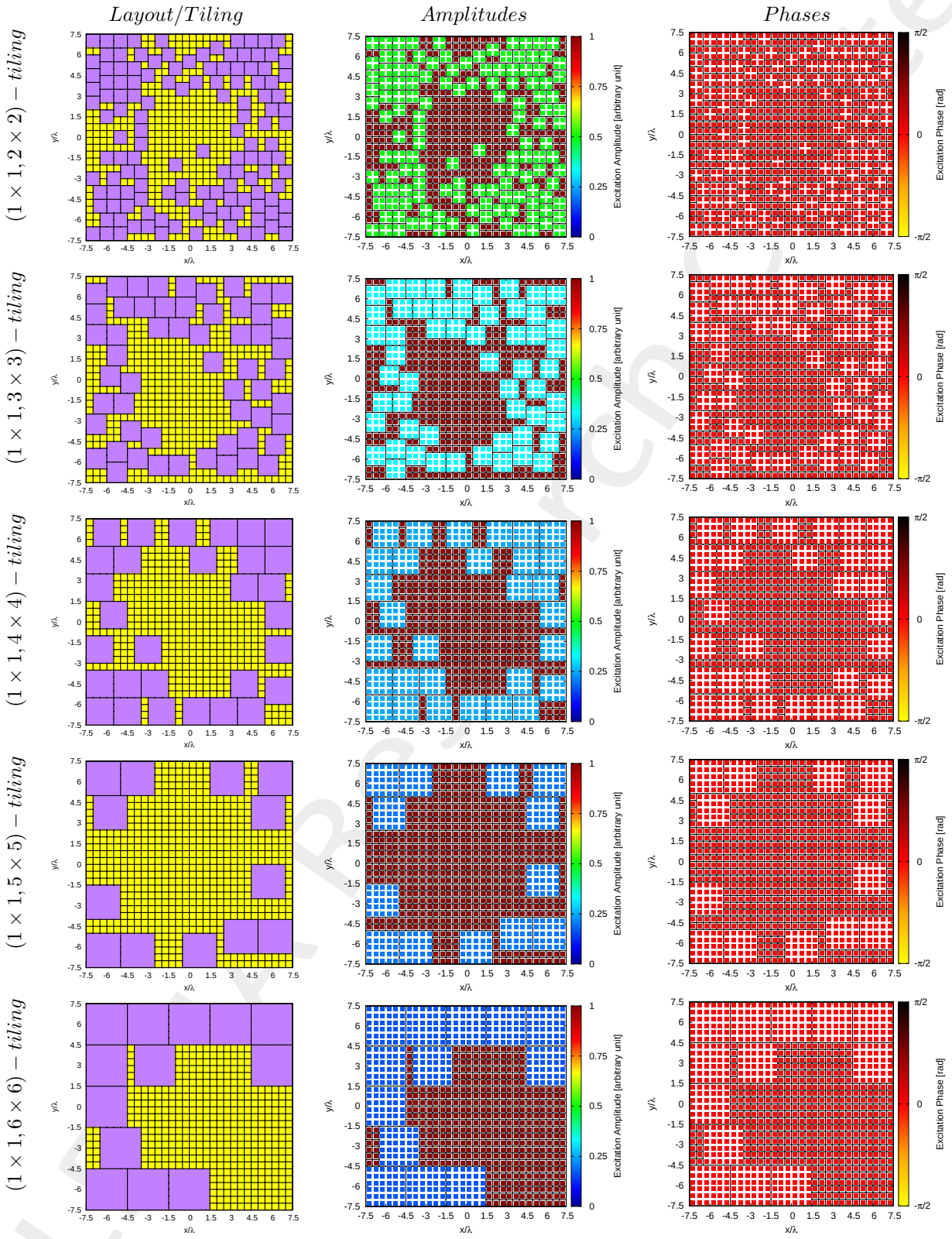

Figure 24: Numerical Assessment ($d_x = d_y = 0.5$ [λ], $k = 30$, $q = 30$, $J = 900$) - Tiling configuration and weights coefficients value.

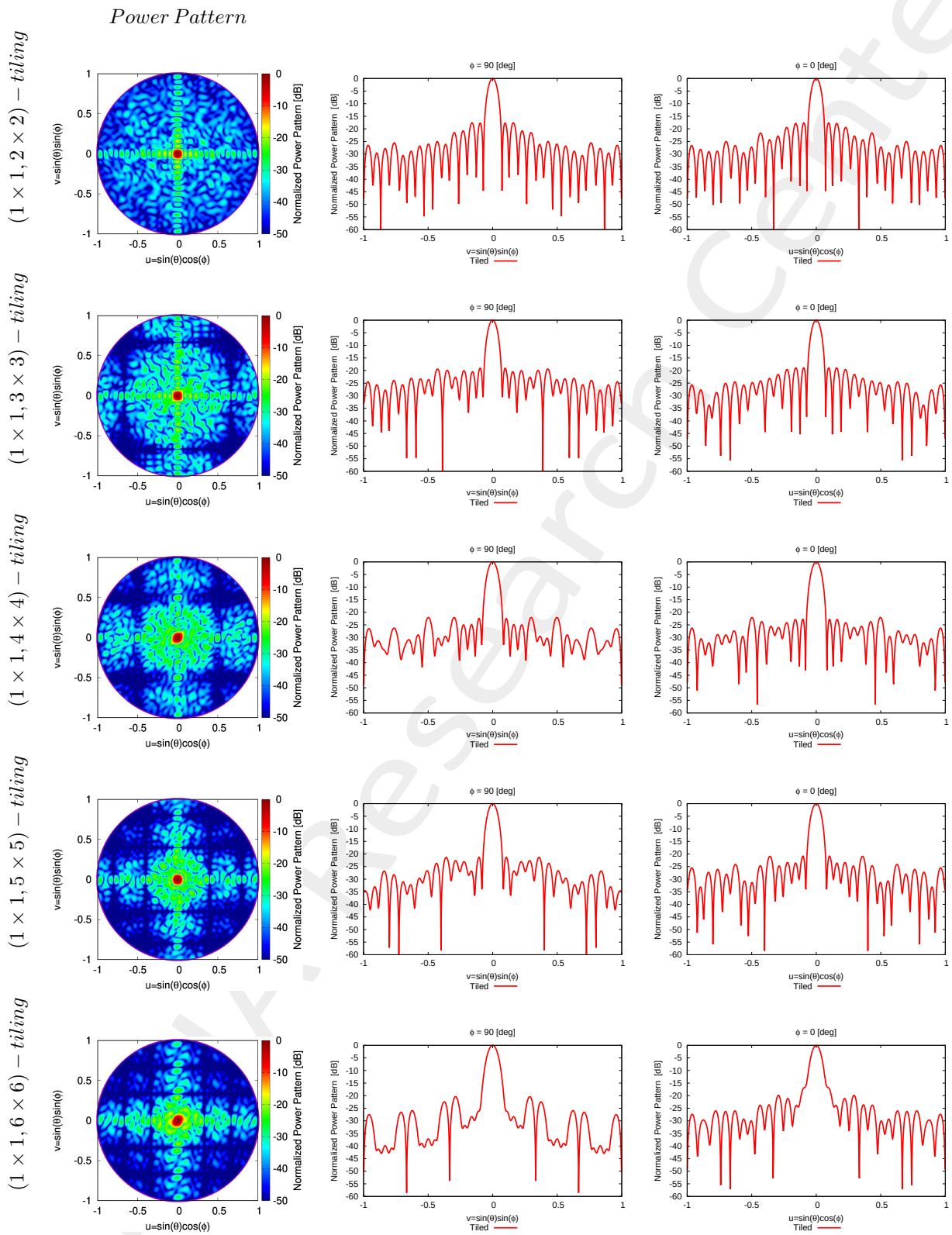

Figure 25: Numerical Assessment ($d_x = d_y = 0.5$ [λ], $k = 30$, $q = 30$, $J = 900$) - Power patterns of the solutions.

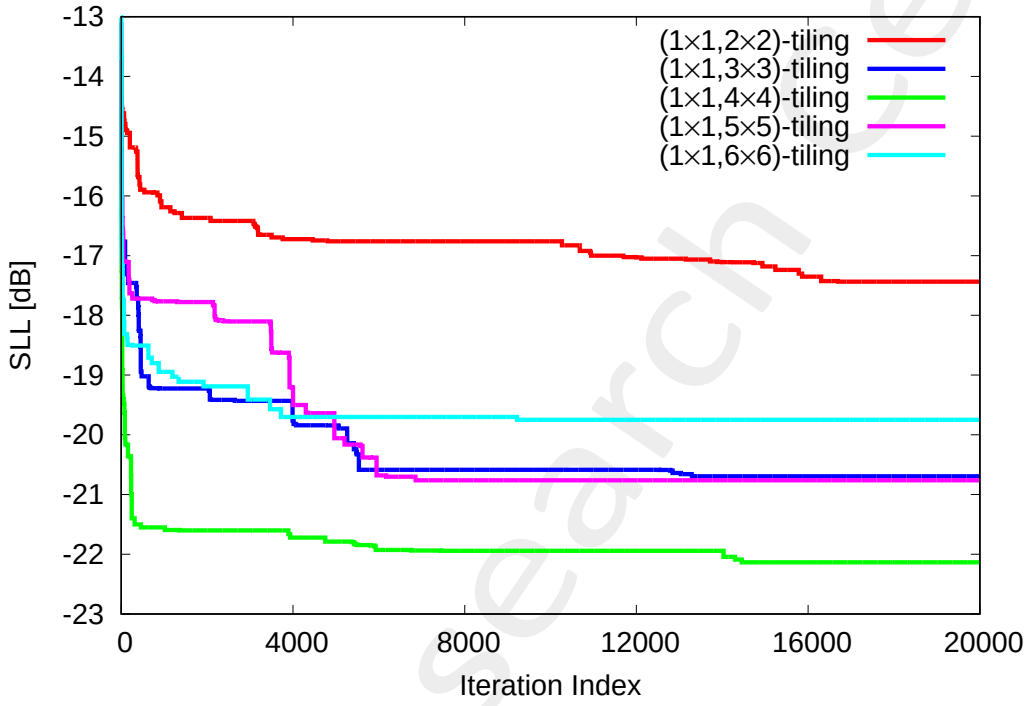

Figure 26: Numerical Assessment ($d_x = d_y = 0.5$ [λ], $k = 30$, $q = 30$, $J = 900$) - SLL vs. Iterations.

	SLL [dB]	D [dBi]	$HPBW_{az}$ [deg]	$HPBW_{el}$ [deg]	TRM
$(1 \times 1, 2 \times 2) - tiling$	-18.15	33.79	3.55	3.55	516
$(1 \times 1, 3 \times 3) - tiling$	-20.65	33.13	3.68	3.66	476
$(1 \times 1, 4 \times 4) - tiling$	-22.12	32.88	3.86	3.94	465
$(1 \times 1, 5 \times 5) - tiling$	-20.76	33.14	3.78	3.80	588
$(1 \times 1, 6 \times 6) - tiling$	-19.67	32.49	3.89	4.24	445

Table XII: Pattern descriptors for the presented solutions.

4 Conclusions

In the next years phased arrays are expected to be widely used for the new generation of communication systems. The research in this field is pushing towards the study of new design strategies capable of reducing the high production costs of these antennas while providing a simple and effective architecture.

In accordance with market trends, this thesis proposes an innovative modular strategy for the design of planar phased arrays. The presented approach provides a complete and irregular array layout using two square tiles of different sizes. Starting from analysis of covering theorems derived in field of mathematics, an enumerative approach , the ETM, able to retrieve the optimal tiling while providing the total aperture coverage with the best radiation performance has been developed in order to deal with the synthesis of low/medium-size rectangular arrays. Subsequently, a method based on optimization, the OTM, has been developed to address the synthesis of large arrays. Since the cardinality of the problem increases as the aperture of the array increases, the OTM exploits a *smart* coding technique able to provides a substantial reduction of the research space dimension.

The ETM and the OTM have been numerically validated and tested. The numerical analysis is aimed both at the general application level (using non-isophoric excitations) and in the specific field of satellite communications (using isophoric excitations).

Evidence

- Thanks to the exhaustive exploration of the solutions space, the ETM method is able to find the optimal solution (or a set of optimal solutions, MOPs) that provides the minimum/maximize the desired objective (or objectives, MOPs). Furthermore, the total coverage of the surface is guaranteed by covering mathematical theory and the relative generalization;
- The coding used for the representation of the solutions/tilings in the OTM allows a substantial reduction of the research space. As a result, the large array synthesis that was computationally intractable is now affordable;

Conclusions w.r.t. Clustered Arrays State of Art

With respect to *classical* clustering techniques which uses subarrays with arbitrary unconstrained shapes the proposed modular strategy ensures a simpler yet low cost antenna system. In fact, the “traditional” unconstrained clusters shapes do not guarantee to be physically contiguous and the associated feeding network can potentially become very complex and expensive.

Whereas, in comparison with the state of the art of tiled arrays, the following outcomes are stated:

1. The presented square-tiling approach, guarantees the optimal tiling of the antenna aperture using the available tiles. I.e. only tiles with predefined geometry has to be manufactured;
2. Unlike single shape tiling approachesin which the number of TRMs is fixed, multiple shapes tilings allows the designer to have control over the number of TRMs. This additional DoF can provide a wider range of candidate solutions;

3. Moreover, multiple shapes tilings approaches enables better performance also in presence of isophoric excitations. This is due to the fact that they can provide more than just one amplitude quantization level (e.g. a set of $m \times m$ and $n \times n$ square tiles yields two amplitude quantization levels), which results is a sort of amplitude tapering;

4. The usage of square tiles seems to enhance the steering performance over tiles with other geometric shapes (e.g. dominoes), at least for small scanning angles;

Future Works

Future work should be aimed at improving the scanning performance of these arrays, as it is the main limiting factor. In this direction it could be interesting to analyze the use of:

- Multiple tiles: Use a set of tiles with more than two sizes in order to have different clustering ratios and multiple amplitude quantization levels, i.e. additional DoFs;
- Phase synthesis: Given the optimal tiling optimize the phase coefficients.
- *Tapered* tiles: Generate subarray pattern able to suppress the arising grating lobes, an thus boosting the scanning performance for a limited FoV. This can be achieved at the price of having a more complex module architecture (feeding network inside the module)*;*
- Partial-subarrayed array: Move some control points at the subarray level while leave other at the element level give more control of the generated pattern;
- Meta-materials;

More information on the topics of this document can be found in the following list of references.

References

[1] P. Rocca, G. Oliveri, and A. Massa, "Differential Evolution as applied to electromagnetics," *IEEE Antennas Propag. Mag.*, vol. 53, no. 1, pp. 38-49, Feb. 2011.

[2] M. Salucci, G. Gottardi, N. Anselmi, and G. Oliveri, "Planar thinned array design by hybrid analytical-stochastic optimization," *IET Microwaves, Antennas & Propagation*, vol. 11, no. 13, pp. 1841-1845, Oct. 2017

[3] P. Rocca, N. Anselmi, A. Polo, and A. Massa, "An irregular two-sizes square tiling method for the design of isophoric phased arrays," *IEEE Trans. Antennas Propag.*, vol. 68, no. 6, pp. 4437-4449, Jun. 2020.

[4] P. Rocca, N. Anselmi, A. Polo, and A. Massa, "Modular design of hexagonal phased arrays through diamond tiles," *IEEE Trans. Antennas Propag.*, vol.68, no. 5, pp. 3598-3612, May 2020.

[5] N. Anselmi, L. Poli, P. Rocca, and A. Massa, "Design of simplified array layouts for preliminary experimental testing and validation of large AESAs," *IEEE Trans. Antennas Propag.*, vol. 66, no. 12, pp. 6906-6920, Dec. 2018.

[6] N. Anselmi, P. Rocca, M. Salucci, and A. Massa, "Contiguous phase-clustering in multibeam-on-receive scanning arrays," *IEEE Trans. Antennas Propag.*, vol. 66, no. 11, pp. 5879-5891, Nov. 2018.

[7] G. Oliveri, G. Gottardi, F. Robol, A. Polo, L. Poli, M. Salucci, M. Chuan, C. Massagrande, P. Vinetti, M. Mattivi, R. Lombardi, and A. Massa, "Co-design of unconventional array architectures and antenna elements for 5G base station," *IEEE Trans. Antennas Propag.*, vol. 65, no. 12, pp. 6752-6767, Dec. 2017.

[8] N. Anselmi, P. Rocca, M. Salucci, and A. Massa, "Irregular phased array tiling by means of analytic schemata-driven optimization," *IEEE Trans. Antennas Propag.*, vol. 65, no. 9, pp. 4495-4510, September 2017.

[9] N. Anselmi, P. Rocca, M. Salucci, and A. Massa, "Optimization of excitation tolerances for robust beamforming in linear arrays," *IET Microwaves, Antennas & Propagation*, vol. 10, no. 2, pp. 208-214, 2016.

[10] P. Rocca, R. J. Mailloux, and G. Toso, "GA-Based optimization of irregular sub-array layouts for wideband phased arrays desig," *IEEE Antennas and Wireless Propag. Lett.*, vol. 14, pp. 131-134, 2015.

[11] P. Rocca, M. Donelli, G. Oliveri, F. Viani, and A. Massa, "Reconfigurable sum-difference pattern by means of parasitic elements for forward-looking monopulse radar," *IET Radar, Sonar & Navigation*, vol 7, no. 7, pp. 747-754, 2013.

[12] P. Rocca, L. Manica, and A. Massa, "Ant colony based hybrid approach for optimal compromise sum-difference patterns synthesis," *Microwave Opt. Technol. Lett.*, vol. 52, no. 1, pp. 128-132, Jan. 2010.

[13] G. Oliveri, A. Gelmini, A. Polo, N. Anselmi, and A. Massa, "System-by-design multi-scale synthesis of task-oriented reflectarrays," *IEEE Trans. Antennas Propag.*, vol. 68, no. 4, pp. 2867-2882, Apr. 2020.

[14] N. Anselmi, L. Poli, P. Rocca, and A. Massa, "Design of simplified array layouts for preliminary experimental testing and validation of large AESAs," *IEEE Trans. Antennas Propag.*, vol. 66, no. 12, pp. 6906-6920, Dec. 2018.

[15] M. Salucci, F. Robol, N. Anselmi, M. A. Hannan, P. Rocca, G. Oliveri, M. Donelli, and A. Massa, "S-Band spline-shaped aperture-stacked patch antenna for air traffic control applications," *IEEE Tran. Antennas Propag.*, vol. 66, no. 8, pp. 4292-4297, Aug. 2018.

[16] M. Salucci, L. Poli, A. F. Morabito, and P. Rocca, "Adaptive nulling through subarray switching in planar antenna arrays," *Journal of Electromagnetic Waves and Applications*, vol. 30, no. 3, pp. 404-414, February 2016

[17] T. Moriyama, L. Poli, and P. Rocca, "Adaptive nulling in thinned planar arrays through genetic algorithms," *IEICE Electronics Express*, vol. 11, no. 21, pp. 1-9, Sep. 2014.

[18] L. Poli, P. Rocca, M. Salucci, and A. Massa, "Reconfigurable thinning for the adaptive control of linear arrays," *IEEE Trans. Antennas Propag.*, vol. 61, no. 10, pp. 5068-5077, Oct. 2013.

[19] P. Rocca, L. Poli, G. Oliveri, and A. Massa, "Adaptive nulling in time-varying scenarios through time-modulated linear arrays," *IEEE Antennas Wireless Propag. Lett.*, vol. 11, pp. 101-104, 2012.

[20] P. Rocca, L. Poli, A. Polo, and A. Massa, "Optimal excitation matching strategy for sub-arrayed phased linear arrays generating arbitrary shaped beams," *IEEE Trans. Antennas Propag.*, vol. 68, no. 6, pp. 4638-4647, Jun. 2020.

[21] G. Oliveri, G. Gottardi and A. Massa, "A new meta-paradigm for the synthesis of antenna arrays for future wireless communications," *IEEE Trans. Antennas Propag.*, vol. 67, no. 6, pp. 3774-3788, Jun. 2019.

[22] P. Rocca, M. H. Hannan, L. Poli, N. Anselmi, and A. Massa, "Optimal phase-matching strategy for beam scanning of sub-arrayed phased arrays," *IEEE Trans. Antennas and Propag.*, vol. 67, no. 2, pp. 951-959, Feb. 2019.

[23] N. Anselmi, P. Rocca, M. Salucci, and A. Massa, "Contiguous phase-clustering in multibeam-on-receive scanning arrays," *IEEE Trans. Antennas Propag.*, vol. 66, no. 11, pp. 5879-5891, Nov. 2018.

[24] L. Poli, G. Oliveri, P. Rocca, M. Salucci, and A. Massa, "Long-Distance WPT Unconventional Arrays Synthesis," *Journal of Electromagnetic Waves and Applications*, vol. 31, no. 14, pp. 1399-1420, Jul. 2017.

[25] G. Gottardi, L. Poli, P. Rocca, A. Montanari, A. Aprile, and A. Massa, "Optimal Monopulse Beamforming for Side-Looking Airborne Radars," *IEEE Antennas Wireless Propag. Lett.*, vol. 16, pp. 1221-1224, 2017.

[26] G. Oliveri, M. Salucci, and A. Massa, "Synthesis of modular contiguously clustered linear arrays through a sparseness-regularized solver," *IEEE Trans. Antennas Propag.*, vol. 64, no. 10, pp. 4277-4287, Oct. 2016.

[27] P. Rocca, G. Oliveri, R. J. Mailloux, and A. Massa, "Unconventional phased array architectures and design Methodologies - A review," *Proceedings of the IEEE = Special Issue on 'Phased Array Technologies', Invited Paper*, vol. 104, no. 3, pp. 544-560, March 2016.

[28] P. Rocca, M. D'Urso, and L. Poli, "Advanced strategy for large antenna array design with subarray-only amplitude and phase contr," *IEEE Antennas and Wireless Propag. Lett.*, vol. 13, pp. 91-94, 2014.

[29] L. Manica, P. Rocca, G. Oliveri, and A. Massa, "Synthesis of multi-beam sub-arrayed antennas through an excitation matching strategy," *IEEE Trans. Antennas Propag.*, vol. 59, no. 2, pp. 482-492, Feb. 2011.

[30] G. Oliveri, "Multi-beam antenna arrays with common sub-array layouts," *IEEE Antennas Wireless Propag. Lett.*, vol. 9, pp. 1190-1193, 2010.

[31] L. T. P. Bui, N. Anselmi, T. Isernia, P. Rocca, and A. F. Morabito, "On bandwidth maximization of fixed-geometry arrays through convex programming," *Journal of Electromagnetic Waves and Applications*, vol. 34, no. 5, pp. 581-600, 2020.

[32] N. Anselmi, L. Poli, P. Rocca, and A. Massa, "Design of simplified array layouts for preliminary experimental testing and validation of large AESAs," *IEEE Trans. Antennas Propag.*, vol. 66, no. 12, pp. 6906-6920, Dec. 2018.

[33] G. Gottardi, L. Poli, P. Rocca, A. Montanari, A. Aprile, and A. Massa, "Optimal Monopulse Beamforming for Side-Looking Airborne Radars," *IEEE Antennas Wireless Propag. Lett.*, vol. 16, pp. 1221-1224, 2017.

[34] G. Oliveri and T. Moriyama, "Hybrid PS-CP technique for the synthesis of n-uniform linear arrays with maximum directivi," *Journal of Electromagnetic Waves and Applications*, vol. 29, no. 1, pp. 113-123, Jan. 2015.

[35] P. Rocca and A. Morabito, "Optimal synthesis of reconfigurable planar arrays with simplified architectures for monopulse radar applications," *IEEE Trans. Antennas Propag.*, vol. 63, no. 3, pp. 1048-1058, Mar. 2015.

[36] A. F. Morabito and P. Rocca, "Reducing the number of elements in phase-only reconfigurable arrays generating sum and difference patterns," *IEEE Antennas and Wireless Propagation Letters*, vol. 14, pp. 1338-1341, 2015.

[37] P. Rocca, N. Anselmi, and A. Massa, "Optimal synthesis of robust beamformer weights exploiting interval analysis and convex optimization," *IEEE Trans. Antennas Propag.*, vol. 62, no. 7, pp. 3603-3612, Jul. 2014.

[38] A. Morabito and P. Rocca, "Optimal synthesis of sum and difference patterns with arbitrary sidelobes subject to common excitations constraints," *IEEE Antennas Wireless Propag. Lett.*, vol. 9, pp. 623-626, 2010.

[39] D. Sartori, G. Oliveri, L. Manica, and A. Massa, "Hybrid design of no-regular linear arrays with accurate control of the pattern sidelobe," *IEEE Trans. Antennas Propag.*, vol. 61, no. 12, pp. 6237-6242, Dec. 2013.